PCCP

ROYAL SOCIETY OF CHEMISTRY

PAPER

View Article Online
View Journal | View Issue

Cite this: *Phys. Chem. Chem. Phys.*, 2022, **24**, 14228

Can domain-based local pair natural orbitals approaches accurately predict phosphorescence energies?†

Giovanna Bruno, [a] Bernardo de Souza,[b] Frank Neese[c] and Giovanni Bistoni *[cd]

Received 7th April 2022,
Accepted 20th May 2022

DOI: 10.1039/d2cp01623k

rsc.li/pccp

Since the discovery of the peculiar conducting and optical properties of aromatics, many efforts have been made to characterize and predict their phosphorescence. This physical process is exploited in modern Organic Emitting Light Diodes (OLEDs), and it is also one of the processes decreasing the efficiency of Dye-sensitized solar cells (DSSCs). Herein, we propose a computational strategy for the accurate calculation of singlet–triplet gaps of aromatic compounds, which provides results that are in excellent agreement with available experimental data. Our approach relies on the domain-based local pair natural orbital (DLPNO) variant of the "gold standard" CCSD(T) method. The convergence of our results with respect to the key technical parameters of the calculation, such as the basis set used, the approximations employed in the perturbative triples correction, and the dimension of the PNOs space, was thoroughly discussed.

1 Introduction

Aromatic compounds constitute about 30% of all the known synthetic and natural organic compounds.[1] Thanks to their peculiar thermodynamic stability, reactivity and physical–chemical properties, they are suitable materials for many industrial, medicinal and engineering applications.

During the first half of the last century, scientists observed that aromatic molecules, either isolated or polymeric, exhibited interesting conducting and absorption properties, which could be exploited for the design of low-cost, easy to fabricate, flexible, green, electrical and emitting devices.[2–5] The first purely organic semiconductor, the charge-transfer complex TTF–TCNQ, whose donor and acceptor moieties are both aromatic (tetrathiafulvalene (TTF) and tetracyano-*p*-quinodimethane (TCNQ)[6]), was proposed in 1973 by J. Ferraris *et al.*[7] In such materials, conduction can be activated by applying a voltage across an electrochemical cell, by doping or by photoexcitation. The latter is also a fundamental step of the dye-sensitized solar cells work-flow,[8] in which an organic or metalorganic dye, usually containing highly conjugated aromatic moieties,[9–16] is excited to a low-lying excited state by absorbing UV-vis or NIR wavelenghts; then, through a relaxing non-radiative process, it injects electrons into the band gap of an inorganic semiconductor, initiating the current flux. Thus, in such a device, radiative relaxation processes, such as fluorescence or phosphorescence, could dramatically decrease the efficiency. In contrast, these radiative processes are the basis for the functioning of OLEDs (Organic Light Emitting Diodes),[17] whose layers are usually made of aromatic polymers or molecules.[18–20]

The ubiquitous importance of aromatic compounds in chemistry stimulated many experimental and computational studies aimed at characterizing their ground state and excited states properties.[21–26] In particular, the low-lying triplet states of aromatic compounds have always attracted the interest of the scientific community due to their unique photophysical and photochemical properties, so that the first extensive experimental work on the topic was carried out by Lewis and Kasha as early as 1944.[27] Since the transition from the first excited triplet state (T_1) to the singlet ground state (S_0) is spin-forbidden, T_1 states have longer lifetimes (up to seconds) than S_1 states (around nanoseconds)[16,21] implying that phosphorescence may persist much longer than fluorescence after excitation. Besides, the probability of formation of triplet excitons, pursuant to electrical excitation, is three times higher than that of singlet excitons,[28,29] making phosphorescent OLEDs usually more efficient than fluorescent ones.[30,31] In addition, although spin-orbit coupling is usually considered to be small in organic compounds, many studies have demonstrated that benzene derivatives and polycyclic aromatic hydrocarbons, conjugated

[a] *Dipartimento di Chimica, Università degli Studi di Milano, via Golgi 19, 20133 Milano, Italy*
[b] *FAccTs GmbH, Köln, Germany*
[c] *Max-Planck-Institut für Kohlenforschung, Kaiser-Wilhelm-Platz 1, D-45470 Mülheim an der Ruhr, Germany*
[d] *Dipartimento di Chimica, Biologia e Biotecnologie, Università di Perugia, Perugia, Italy. E-mail: giovanni.bistoni@unipg.it*

† Electronic supplementary information (ESI) available. See DOI: https://doi.org/10.1039/d2cp01623k

or substituted by pnictogens or chalcogens, still exhibit ultrafast intersystem crossing.[32–36] Triplet states of aromatic compounds can also promote reduction and addiction reactions which are usually highly endothermic in the ground state (S_0).[37–39] The reason of this behavior has been identified with the anti-aromaticity of triplet states.[40–42]

Computational protocols for the prediction of singlet–triplet gaps have been proposed since the end of 90s, based on a plethora of different electronic structure methods. Time-Dependent Density Functional Theory (TDDFT) is of course a popular approach in this context, as it allows the simulation of large molecules and macromolecules in their excited states.[22,43] However, many benchmark studies on organic molecules (including acenes[44]) have emphasized the accuracy limits of popular exchange correlation functionals, especially in the calculation of triplet state energies.[45–52] Thus, several attempts have been made over the years to overcome these limitations of DFT. In particular, double-hybrid functionals[53] demonstrated remarkable accuracy for the calculation of singlet–triplet excitation energies of organic compounds,[54,55] as well as of spin states energies of metalorganic complexes.[56] In contrast, correlated wavefunction-based methods such as Full Configuration Interaction (FULL-CI)[57] and Canonical Coupled Cluster with Single, Double and Perturbative Triple excitations (CCSD(T))[58] have shown great accuracy for small model systems. Unfortunately, due to their steep scaling with the system size, applications of these approaches in their canonical implementation are still limited to small and medium-size molecules. Machine learning techniques, obviously affected by generality issues, have also been recently applied to large datasets[59] of organic molecules to compute phosphorescence energy gaps, yielding errors comparable to DFT ones ($\sim$0.1 eV).[60,61]

In this work, we explore the use of the Domain-Based Local Pair Natural Orbital CCSD(T) method[62,63] (DLPNO-CCSD(T)) for the calculation of phosphorescence energies of aromatics. This method belongs to the family of Local Correlation CCSD(T) approaches,[64–66] which exploit the short-range nature of electron correlation to increase the efficiency of post Hartree-Fock approaches. In particular, we propose two computational protocols based on the DLPNO-CCSD(T) methodology that differ in their accuracy and computational cost: (i) ''Gold'' settings are designed to provide results that are at convergence with respect to both the basis set size and the DLPNO thresholds used, and thus retain essentially canonical CCSD(T) accuracy; (ii) ''Silver'' settings provide the optimal balance between accuracy and computational cost for large systems, thus allowing the calculation phosphorescence energies for systems with potentially hundreds of atoms.

The manuscript is organized as follows. Computational details are given in Section 2.3. In Section 3.1, the convergence of the DLPNO-CCSD(T) energy of aromatic molecules in their singlet and triplet states with respect to the key technical parameters of the calculation is studied in detail. This information is then used for defining the Gold and Silver DLPNO-CCSD(T) settings. In Section 3.2, these settings are used to compute adiabatic singlet–triplet gaps of a series of aromatic molecules, and their accuracy is verified using experimental data as reference. In Section 3.3, our Silver methodology is used to compute the key photophysical properties of challenging carbazolyl dicyanobenzene (CDCB) compounds as an illustrative example of its potentially broad applicability.

2 Computational details

2.1 Experimental reference data

The reference experimental phosphorescence energies were mainly taken from the work by Lewis and Kasha[27] and partly from the works by Siebrand[67] and by Metcalfe *et al.*[68] The entire set consists of about 100 aromatic compouds. Among those, we selected 18 compounds trying to maximize the sample's variance with respect to chemical structure. Therefore, our sample includes benzene derivatives (Group A), naphthalene derivatives (Group B), polycyclic aromatic hydrocarbons (Group C), a group named by us ''complex conjugated compounds'' (Group D), which are mainly biphenyl derivatives, and heterocycles (Group E) (Fig. 1).

2.2 Methodological aspects

The theoretical phosphorescence energy, corresponding to the adiabatic singlet–triplet gap (ΔE_{00}), was computed by adding the differential zero-point energy correction (ΔZPE) to the ''well to well'' singlet–triplet gap (ΔE) (eqn (1)) computed at various levels of electronic structure theory.

$$\Delta E_{00} = \Delta E + \Delta ZPE \quad (1)$$

In particular, we shall introduce two computational protocols for the calculation of singlet–triplet gaps of aromatics that rely on the DLPNO-CCSD(T) methodology for the calculation of ΔE. Unless otherwise specified, all calculations were carried out with a development version of ORCA based on ORCA 4.2.1.[69]

2.3 Computational details

2.3.1 Geometry optimizations. Geometry optimizations were carried out at the DFT level of theory. To select a suitable exchange correlation functional, we optimized both the singlet and the triplet state of all compounds in Fig. 1 using the BLYP, B3LYP and M06-2X functionals. The Grimme's D3 dispersion correction[70–72] was included in all the calculations. In particular, the original zero-damping correction D3(0) (D3ZERO keyword of ORCA 4.2.1) was employed for M06-2X optimizations while the Becke-Johnson damping variant (D3BJ keyword of ORCA 4.2.1) was employed for both BLYP and B3LYP optimizations. The optimized geometries were then used to perform DLPNO-CCSD(T) single point calculations. Our analysis (see Section S1 of ESI,† for further details) revealed that, in most of the cases, B3LYP optimized geometries provide the lowest singlet ground state (S_0) and first excited triplet state (T_1) DLPNO-CCSD(T) energies. These data are consistent with those previously published on acenes,[73,74] showing a good agreement between B3LYP structures and both experimental and CCSD(T) structures.

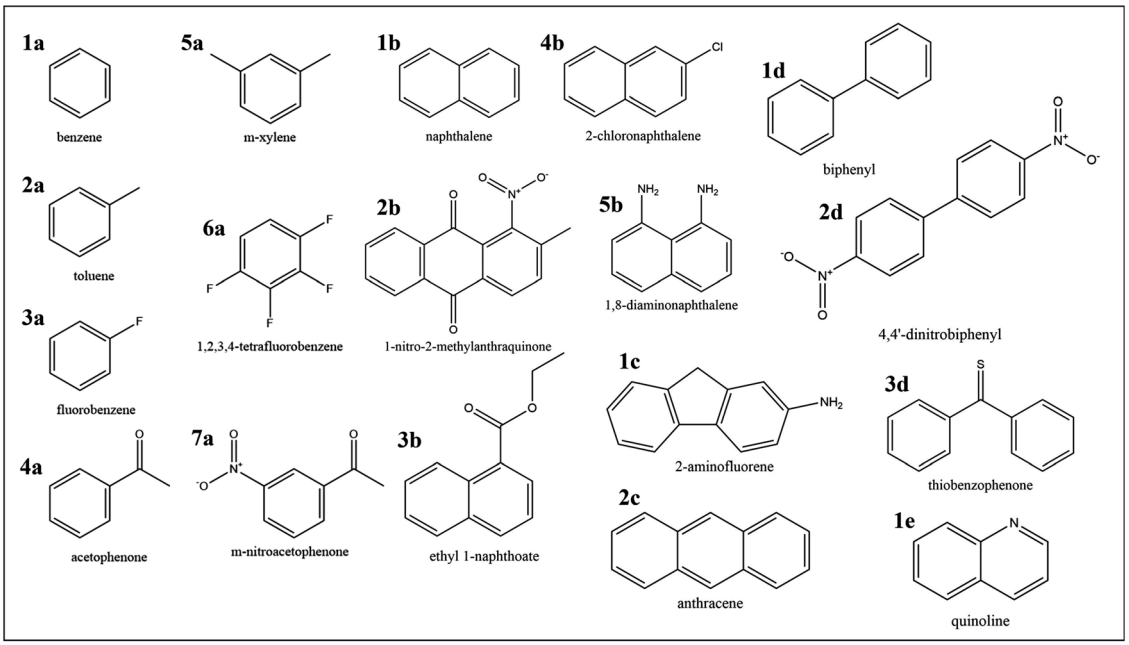

GROUP A: **1a**:benzene; **2a**:toluene; **3a**:fluorobenzene; **4a**:acetophenone; **5a**:m-xylene; **6a**:1,2,3,4-tetrafluorobenzene; **7a**: m-nitroacetophenone.

GROUP B: **1b**:naphthalene; **2b**:2-chloronaphthalene; **3b**:1-nitro-2-methylanthraquinone; **4b**:1,8-diaminonaphthalene; **5b**:ethyl 1-nahthoate.

GROUP C: **1c**:2-aminofluorene; **2c**:anthracene.

GROUP D: **1d**: biphenyl; **2d**:4,4'-dinitrobiphenyl; **3d**:thiobenzophenone.

GROUP E: **1e**:quinoline.

Fig. 1 Sample of Aromatic Compounds GROUP A: **1a**:benzene; **2a**:toluene; **3a**:fluorobenzene; **4a**:acetophenone; **5a**:*m*-xylene; **6a**:1,2,3,4-tetrafluorobenzene; **7a**: *m*-nitroacetophenone. GROUP B: **1b**:naphthalene; **2b**:2-chloronaphthalene; **3b**:1-nitro-2-methylanthraquinone; **4b**:1,8-diaminonaphthalene; **5b**:ethyl 1-nahthoate. GROUP C: **1c**:2-aminofluorene; **2c**:anthracene. GROUP D: **1d**:biphenyl; **2d**:4,4'-dinitrobiphenyl; **3d**:thiobenzophenone. GROUP E: **1e**:quinoline.

Therefore, in our final computational protocols, we employ the B3LYP-D3 functional in conjuction with the def2-TZVPP basis set. The RI approximation for both Coulomb (J) and Exchange (K) integrals (RIJK option of ORCA 4.2.1[75])[76,77] was used to speed up the calculations. Numerical frequencies at the same level of theory were computed to get the zero-point energy (*ZPE*) correction used in the calculation of the adiabatic phosphorescence gap (ΔE_{00}). In all cases and for all molecules real vibrational frequencies were obtained, confirming that the B3LYP optimized geometries correspond to local minima.

2.3.2 DLPNO-CCSD(T) calculations. The open-shell implementation of DLPNO-CCSD(T) method[78,79] was employed for running single-point energy calculations of both the singlet ground state and the first excited triplet state on the corresponding DFT optimized structures, using the Quasi Restricted Orbital (QRO) determinant as the reference wave function. In fact, the transformation of Unrestricted Hartree-Fock (UHF) Canonical Orbitals into Quasi Restricted Orbitals[80,81] allows to avoid a severe spin contamination by returning a zeroth-order wave function which is eigenfunction of $\hat{S}^2$ operator. The RIJK approximation was used to speed up the calculations. The dependence of the DLPNO-CCSD(T) results on the technical parameters of the calculation, such as the basis set, the DLPNO thresholds and the approximations used in the triples correction evaluation, was assessed to define the computational protocols.

With respect to the triples correction evaluation, the (T0) and (T1) corrections were tested in DLPNO calculations. The abbreviation (T0) denotes the traditional semi-canonical perturbative triples correction,[65,82] while (T1) denotes the recently implemented iterative algorithm.[83] The latter is computationally more demanding but returns more accurate results by iteratively calculating triples amplitudes.

In the basis set convergence study, the correlation-consistent basis sets of Dunning[84] (*i.e.*, cc-pVNZ) as well as their "augmented" counterparts (*i.e.*, aug-cc-pVNZ) featuring additional diffuse functions[85] were used. Thus, DLPNO-CCSD(T) single point calculations were performed by increasing the basis set cardinality (N = D, T, Q) of both the cc-pVNZ and aug-cc-pVNZ family. The extrapolation to the complete basis set (CBS) limit for each basis set class was carried out using a two-point extrapolation scheme for both the SCF and

the correlation energy. For the SCF energy, the Karton and Martin's formula[86] (eqn (2a)), also used by Zhong *et al.*,[87] was used. For the correlation energy instead, Truhlar's version[88] of the Helgaker formula[89,90] (eqn (2b)) was employed.

$$E_{\mathrm{SCF}}^{X} = E_{\mathrm{SCF}}^{\mathrm{CBS}} + A\mathrm{e}^{-\alpha\sqrt{X}} \quad (2a)$$

$$E_{\mathrm{corr}}^{\mathrm{X}} = E_{\mathrm{corr}}^{\mathrm{CBS}} + AX^{-\beta} \quad (2b)$$

In particular, $E_{\mathrm{SCF}}^{\mathrm{CBS}}$ and $E_{\mathrm{corr}}^{\mathrm{CBS}}$ were obtained by using 3-ζ and 4-ζ basis sets in combination with α and β parameters calibrated by Neese and Valeev[91] for the 3/4 extrapolation (α = 5.79, β = 3.05). In the following, cc-pVNZ basis sets (N = D, T, Q) are sometimes abbreviated as ''NZ'' for the sake of simplicity, while aug-cc-pVNZ basis sets are denoted as ''aNZ''.

Related to the convergence of the DLPNO-CCSD(T) energies as a function of the DLPNO thresholds, two main parameters were considered: (i) T_{CutPNO}, which determines the pair natural orbitals included in the virtual space of each electron pair while solving the coupled cluster equations (PNOs with occupation numbers lower than the set threshold are discarded); (ii) T_{CutPairs}, which determines the electron pairs included in the coupled cluster treatment (only those whose MP2 correlation energy is higher than the set threshold are included in the Coupled Cluster calculation). In particular, two recent studies by Altun *et al.*[92,93] on the GMTKN55 superset[94] showed that DLPNO-CCSD(T) accuracy can be considerably improved by extrapolating to the complete PNOs space limit (CPS), using the simple two points extrapolation scheme reported in eqn (3):

$$E = E^{X} + F\cdot(E^{Y} - E^{X}) \quad (3)$$

in which E^X and E^Y represent the energies obtained at $T_{\mathrm{CutPNO}} = 10^{-X}$ and $T_{\mathrm{CutPNO}} = 10^{-Y}$ levels, respectively ($Y = X + 1$) and F is a parameter that minimizes the deviation from the canonical CCSD(T) energy. In particular, we followed the procedure proposed by Altun *et al.*[92] by using the pair X = 6 and Y = 7 and the optimal value F = 1.5. This approach is denoted hereafter as CPS(6/7).

2.4 Phosphorescence spectra and rate constants

For the calculation of phosphorescence rates and spectra, the path integral approach implemented in the ORCA_ESD module was used.[95,96] It relies on the harmonic approximation to propagate the time evolution of the systems analytically, but has the advantage to exactly include temperature effects and is able to also include vibronic coupling to the transition dipole moments, which is a key factor for organic molecules without heavy atoms. The method essentially needs the well to well singlet–triplet gap ($T_1 \rightarrow S_0$) ΔE, obtained here from DLPNO-CCSD(T), to compute both the spectrum and the rate constant, together with the oscillator strengths, which were computed using SOC-TDDFT. We performed these excited state calculations using B3LYP with RIJCOSX[97] in combination with def2-TZVPP basis set, LR-CPCM[98] under equilibrium conditions to include the toluene solvation effects and the RI-SOMF(1X)[99] method for the spin-orbit coupling related integrals. The temperature of the simulations was set to 77 K and we used the Silver DLPNO-CCSD(T) ΔE calculated prior to it.

3 Results and discussion

3.1 The ''Gold'' and ''Silver'' DLPNO-CCSD(T) Settings

3.1.1 Accuracy target and design philosophy. In 2009 Hajgató and co-workers tested the performance of canonical CCSD(T) on a small group of polycyclic aromatic hydrocarbons, including benzene, naphthalene and anthracene (compounds **1a**, **1b** and **2c** of Fig. 1). They showed that CCSD(T) phosphorescence energies at the estimated CBS limit deviate from the experimental results of about 0.14 eV for these small acenes.[58,100,101] This is set as the target accuracy for the two protocols developed in this section. To achieve this aim, Gold settings were developed by selecting the technical parameters of the calculations in such a way that the individual errors associated with these parameters were smaller than 0.04 eV. Comparatively less ''tight'' parameters were selected while defining the Silver settings. In this case, errors up to 0.09 eV were considered as acceptable. This study was performed on a subset of three compounds (benzene (**1a**), 1,2,3,4-tetrafluorobenzene (**6a**) and thiobenzophenone (**3d**)) (Fig. 1), which was selected trying to maximize the variance with respect to the chemical structure. In particular, we chose to include compounds of different size and with and without heteroatoms. The results of this study are discussed in the following subsections.

3.1.2 Basis set convergence study. We initially tested the convergence of DLPNO-CCSD(T) energies with respect to the basis set size for the singlet ground state (S_0) and for the first triplet excited state (T_1) of the systems discussed above. For these calculations, we used TightPNO[62,102] settings and the recently published iterative algorithm for the perturbative triples (T1),[83] as implemented in ORCA 4.2.1.

In Fig. 2, we report the basis set convergence plots for the S_0 and T_1 energies, alongside with that of ΔE (Eqn 1) for compound **3d**. Analogous plots for compounds **1a** and **6a** are reported in Section S3 of ESI.† All the relevant energies are reported in Table 1.

Interestingly, by increasing the dimension of the basis set, the singlet–triplet gap increases. Thus, improving the quality of the simulation returns a more endothermic description of the process. Remarkably enough, both the absolute energies and the gap smoothly converge to essentially the same values upon CBS extrapolation, irrespective of the basis set family used. In addition, the variance of the cc-pVNZ gap with respect to N is smaller than that associated with the aug-cc-pVNZ gap. Hence, in the case of cc-pVNZ basis set family, the increase of cardinality affects the gap to a lesser extent.

In order to select the best basis set for the Gold and the Silver protocols, we analysed both the accuracy and the computational cost associated with each basis set. We used the ΔE values extrapolated to the complete basis set limit of the aug-cc-pVNZ family (aTZ/aQZ) as reference to evaluate the error

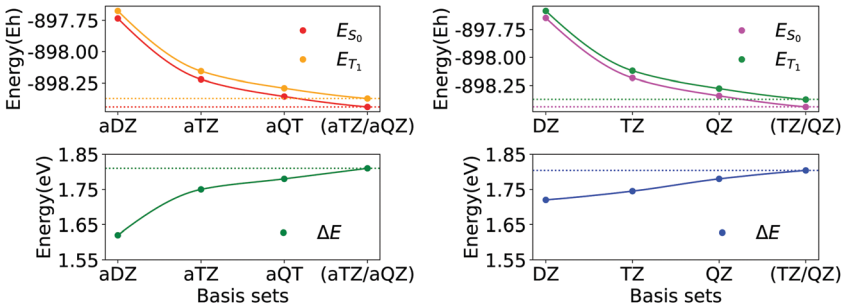

Fig. 2 Basis set convergence of singlet state (E_{S0}), triplet state (E_{T1}) and ΔE gap of compound **3d** (Fig. 1) for basis sets family aug-cc-pVNZ (N = D, T, Q) and for basis sets family cc-pVNZ (N = D, T, Q). Horizontal dotted lines represent energies extrapolated by means of eqn (2a) and (2b).

Table 1 Well to well singlet–triplet gap ($T_1 \rightarrow S_0$, ΔE) (values in eV) of compounds **1a**, **6a** and **3d** (Fig. 1) obtained by employing aug-cc-pVNZ and cc-pVNZ basis sets family (N = D, T, Q) and by extrapolating to the corresponding complete basis set limit (aTZ/aQZ) for aug-cc-pVNZ family and (TZ/QZ) for cc-pVNZ family. All the simulations have been performed by employing T1 and TightPNO options of ORCA 4.2.1

Compounds	Basis sets	ΔE
1a	(aug)/cc-pVDZ	(3.38) 3.87
	(aug)/cc-pVTZ	(3.94) 3.95
	(aug)/cc-pVQZ	(3.97) 3.96
	(aug)/(TZ/QZ)	(3.99) 3.99
6a	(aug)/cc-pVDZ	(3.29) 3.44
	(aug)/cc-pVTZ	(3.43) 3.46
	(aug)/cc-pVQZ	(3.47) 3.48
	(aug)/(TZ/QZ)	(3.50) 3.50
3d	(aug)/cc-pVDZ	(1.62) 1.72
	(aug)/cc-pVTZ	(1.75) 1.75
	(aug)/cc-pVQZ	(1.79) 1.78
	(aug)/(TZ/QZ)	(1.81) 1.80

obtained with smaller basis sets. The corresponding energy differences are shown in Fig. 3.

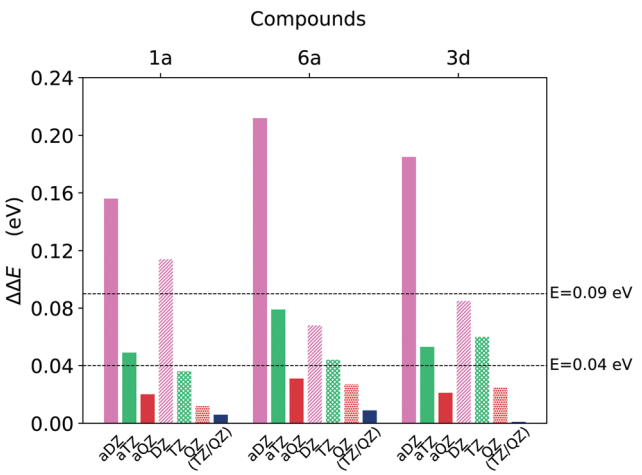

Fig. 3 Basis set incompleteness error associated with DLPNO-CCSD(T) well to well singlet–triplet gap ($T_1 \rightarrow S_0$) ΔE calculations for compounds **1a**, **6a** and **3d** (Fig. 1), obtained for different basis sets and extrapolation schemes. The gap computed at the CBS(aTZ/aQZ) limit was used as reference.

The accuracy of the aug-cc-pVDZ basis set is not satisfactory inasmuch as the deviation from the (aTZ/aQZ) limit ranges from around 0.15 eV to around 0.22 eV. The performances of the cc-pVDZ basis set are slightly better since the deviation remains below 0.09 eV for two of the three compounds analysed. On the contrary, the error associated with basis sets of cardinality N = T and N = Q is always smaller than 0.08 eV and 0.03 eV, respectively, for both the cc-pVNZ and aug-cc-pVNZ basis set families.

In terms of efficiency, the analysis of the computation time in terms of CPU hours (Fig. 4) revealed that, by increasing the cardinality from N = T to N = Q, the computational cost of the calculations increases by 3–4 times for all compounds.

Importantly, the use of diffuse functions in the aug-cc-pVNZ increases dramatically the computational cost with respect to that obtained with the cc-pVNZ family. For example, the computational times associated with the aug-cc-pVQZ basis set are roughly twice the sum of that obtained with cc-pVTZ

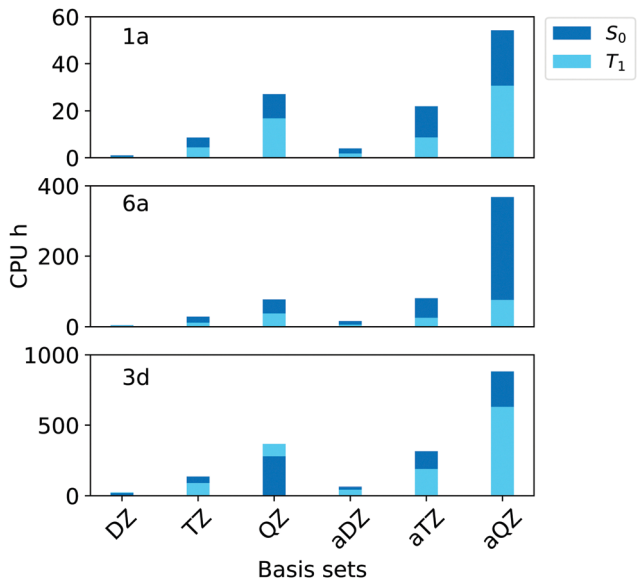

Fig. 4 Computation times in CPU hours for the simulation of singlet (S_0, blue bars) and triplet state (T_1, light blue bars) of compounds **1a**, **6a** and **3d** (Fig. 1) corresponding to aug-cc-pVNZ and cc-pVNZ basis sets family (N = D,T,Q) in combination with T1 and TightPNO options of ORCA 4.2.1.

Table 2 Well to well singlet–triplet gap ($T_1 \rightarrow S_0$) ΔE (values in eV) of compounds **1a**, **6a** and **3d** (Fig. 1) obtained by employing different $T_{CutPNO} = 10^{-X}$ settings (X = 6, 7) and at the (CPS(6/7)) limit, using different levels of theory (DLPNO-CCSD, DLPNO-CCSD(T0) and DLPNO-CCSD(T1)). All calculations were performed by using aug-cc-pVTZ basis set and TightPNO settings for all the DLPNO thresholds besides T_{CutPNO}

Compounds	$T_{CutPNO} = 10^{-X}$	ΔE	$\Delta E^{(T_0)}$	$\Delta E^{(T_1)}$
1a	X = 6	3.88	3.91	3.95
	X = 7	3.88	3.90	3.94
	(6/7)	3.88	3.89	3.93
6a	X = 6	3.37	3.43	3.44
	X = 7	3.36	3.41	3.42
	(6/7)	3.35	3.40	3.41
3d	X = 6	1.65	1.73	1.76
	X = 7	1.66	1.72	1.75
	(6/7)	1.67	1.72	1.75

and cc-pVQZ basis sets. These results demonstrate that cc-pVTZ/cc-pVQZ extrapolation provides ΔE that are at convergence with the basis set size while being at the same time computationally affordable. Thus, this scheme was selected for our "Gold" protocol. For our "Silver" protocol, the cc-pVTZ was used. This basis set provides errors that are below our chosen threshold of 0.09 eV while reducing the the computation time by 55–75% with respect to the corresponing aug-cc-pVTZ basis set.

3.1.3 Perturbative triples effect. Table 2 shows the ΔE values computed at DLPNO-CCSD, DLPNO-CCSD(T0) and DLPNO-CCSD(T1) levels obtained with $T_{CutPNO} = 10^{-6}$, $T_{CutPNO} = 10^{-7}$ and CPS(6/7).

For these systems, the triples contributions to the gap appear to be rather small. Regardless of the T_{CutPNO} value used, the deviation between DLPNO-CCSD and DLPNO-CCSD(T0/T1) is always below 0.09 eV. Only for compound **3d** the contribution of the triples becomes significant, reaching up to 0.11 eV. Hence, it is not surprising that the difference between the DLPNO-CCSD(T0) and the DLPNO-CCSD(T1) results is even smaller, remaining below 0.04 eV in all cases. Interestingly, a noteworthy difference exists between T0 and T1 triples algorithms in terms of efficiency, as shown in Fig. 5.

The computational cost of a DLPNO-CCSD(T0/T1) calculation for these systems increases by 3–5 times with T1. Based on these results, the T0 algorithm was selected for the Silver settings, while the more robust T1 triples correction is used in Gold settings.

3.1.4 DLPNO thresholds convergence study. As shown in Table 2, the effect of T_{CutPNO} threshold on the ΔE energies is also relatively small. In all cases, the deviation between $T_{CutPNO} = 10^{-6}$, $T_{CutPNO} = 10^{-7}$ and CPS(6/7) results remains below 0.04 eV for all compounds.

In terms of efficiency, the computation times associated with $T_{CutPNO} = 10^{-6}$, $T_{CutPNO} = 10^{-7}$ and CPS(6/7) calculations are shown in Fig. 6.

Interestingly, as $T_{CutPNO} = 10^{-6}$ calculations are extremely efficient, the overall computational cost of CPS(6/7) is only slightly higher than that associated with $T_{CutPNO} = 10^{-7}$. Based on these results, we decided to use the extrapolation technique for the treatment of PNOs virtual space in the Gold settings. For the Silver methodology, we decided to set T_{CutPNO} to an

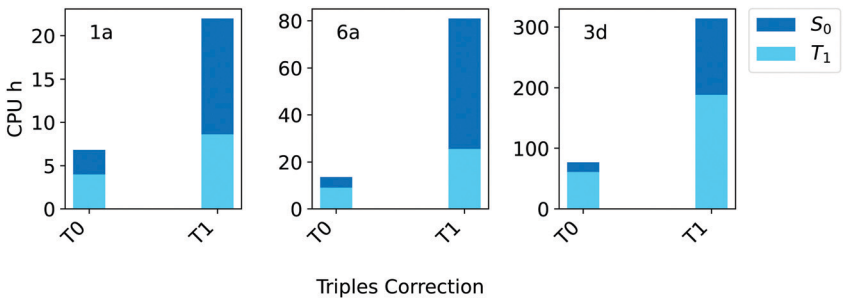

Fig. 5 Computation times in CPU hours for DLPNO-CCSD(T) calculations of the singlet (S_0, blue bars) and triplet state (T_1, light blue bars) of compounds **1a**, **6a** and **3d** (Fig. 1) corresponding to T0 and T1 triples corrections. In all cases, the aug-cc-pVTZ basis set and TightPNO settings were used.

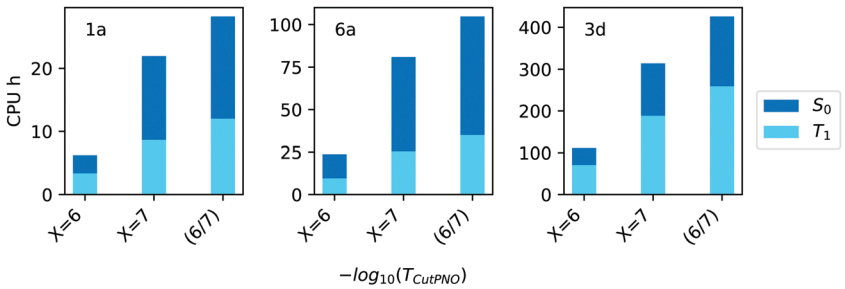

Fig. 6 Computation times in CPU hours for the calculation of singlet (S_0, blue bars) and triplet state (T_1, light blue bars) of compound **1a**, **6a** and **3d** (Fig. 1) with different $T_{CutPNO} = 10^{-X}$ thresholds as well as with CPS(6/7) extrapolation.

Table 3 Technical parameters defining the Gold and Silver DLPNO-CCSD(T) Settings. The corresponding average computation time in CPU hours for compounds **1a**, **6a** and **3d** of Fig. 1 is also shown. The label (TZ/QZ) refers to the CBS extrapolation with cc-pVTZ and cc-pVQZ basis sets. CPS(6/7) refers to the PNO extrapolation technique. See text for details

Method	Basis set	Triples correction	T_{CutPNO}	T_{CutPairs}	t
Gold DLPNO-CCSD(T)	CBS(TZ/QZ)	T1	CPS(6/7)	10^{-5}	562
Silver DLPNO-CCSD(T)	cc-pVTZ	T0	3.33×10^{-7}	10^{-4}	8

intermediate value between 10^{-6} and 10^{-7}, as both thresholds provided similar accuracy. Specifically, we set $T_{\mathrm{CutPNO}} = 3.33 \times 10^{-7}$, corresponding to the default value of DLPNO-CCSD(T) calculations.

Finally, we also investigated the convergence of the results with respect to the T_{CutPairs} parameter. Three thresholds were tested: $T_{\mathrm{CutPairs}} = 10^{-4}$, $T_{\mathrm{CutPairs}} = 10^{-5}$ and $T_{\mathrm{CutPairs}} = 10^{-6}$. In all cases, the aug-cc-pVTZ basis set was used in conjuction with the T1 triples correction and $T_{\mathrm{CutPNO}} = 10^{-7}$. It was found that the results are weakly affected by the specific value used for T_{CutPairs} parameter, with maximum deviations below 0.02 eV. The computational cost associated with the calculations is also comparable. For these reasons, we selected the $T_{\mathrm{CutPairs}} = 10^{-4}$ threshold for the Silver settings, and the more conservative $T_{\mathrm{CutPairs}} = 10^{-5}$ threshold for the Gold settings. These correspond to the default thresholds of NormalPNO and TightPNO calculations, respectively.

3.1.5 Summary: gold *vs.* silver settings. In this section we discussed the accuracy and efficiency of the DLPNO-CCSD(T) methodology for the calculation of ΔE of aromatics in relation to the technical parameters of the calculation. This study led to the definition of two computational settings for DLPNO-CCSD(T) calculations in this context, namely the ''Gold'' and ''Silver'' settings. The former is an accurate procedure which can be considered as our gold standard. The second is a cost effective procedure applicable to large systems. The parameters combination and the average computation time ($\bar{t}$) for both the methodologies are summarized in Table 3.

3.2 Computed *vs* experimental phosphorescence energies

In this section, we analyse the agreement between the experimental and theoretical phosphorescence gap for the compounds reported in Fig. 1.

Table 4 reports the ΔE_{00} values computed using the Silver and the Gold DLPNO-CCSD(T) settings for the calculation of ΔE; it also reports the corresponding UHF and QRO energies ($E(0)$, which is expected to be close to the corresponding Restricted Open Hartree-Fock (ROHF) energy), as well as the experimental phosphorescence gap and the differential zero-point energy correction (ΔZPE).

The mean absolute error associated to the UHF and $E(0)$ references is extremely high, though the transformation of the UHF canonical orbitals into quasi-restricted orbitals markedly improves the accuracy.

Remarkably enough, DLPNO-CCSD and the DLPNO-CCSD(T) perform equally well, with errors of the order of few tenths of eV. Importantly, the mean absolute error (MAE) of Gold DLPNO-CCSD(T) is the same of the canonical CCSD(T) one (0.14 eV) reported by Hajgató and co-workers.[58] In addition, the accuracy of the Silver and Gold methodologies is

Table 4 DLPNO-CCSD(T) adiabatic singlet–triplet gap (ΔE_{00}) computed using Gold and Silver (values in parenthesis) Settings for the compounds reported in Fig. 1. The corresponding *ZPE*-corrected UHF and QRO energies ($E(0)$) are also shown for comparison, alongside with the differential zero-point energy correction (ΔZPE) and the experimental singlet–triplet gap (E_{exp}) in eV

	ΔE_{00}					
Compounds	UHF	$E(0)$	DLPNO-CCSD	DLPNO-CCSD(T)	ΔZPE	E_{exp}
1a	2.51 (2.51)	3.80 (3.81)	3.70 (3.66)	3.76 (3.69)	−0.22	3.66[b]
2a	2.44 (2.45)	3.72 (3.72)	3.61 (3.58)	3.67 (3.61)	−0.20	3.58
3a	2.54 (2.55)	3.79 (3.80)	3.70 (3.66)	3.76 (3.70)	−0.21	3.65[b]
4a	1.70 (1.69)	2.74 (2.74)	3.18 (3.11)	3.25 (3.15)	−0.10	3.30
5a	2.38 (2.38)	3.64 (3.65)	3.53 (3.51)	3.59 (3.53)	−0.18	3.52[b]
6a	5.25 (2.25)	3.11 (3.13)	3.32 (3.29)	3.39 (3.35)	−0.10	3.62[b]
7a	1.39 (1.32)	2.49 (2.40)	2.88 (2.82)	2.87 (2.84)	−0.11	2.65
1b	2.04 (2.05)	2.90 (2.90)	2.73 (2.71)	2.72 (2.67)	−0.14	2.64
2b	0.59 (0.57)	1.59 (1.56)	2.79 (2.71)	3.01 (2.88)	−0.08	2.69
3b	1.82 (1.82)	2.59 (2.59)	2.54 (2.54)	2.55 (2.54)	−0.20	2.49
4b	1.99 (1.99)	3.02 (3.03)	2.74 (2.74)	2.73 (2.71)	−0.14	2.60
5b	1.84 (1.87)	2.77 (2.79)	2.44 (2.44)	2.43 (2.40)	−0.15	2.37
1c	2.05 (2.03)	3.32 (3.49)	3.00 (3.01)	3.00 (2.99)	−0.13	2.81
2c	1.24 (1.24)	1.81 (1.81)	1.93 (1.93)	1.95 (1.95)	−0.10	1.85[a]
1d	2.04 (2.05)	3.44 (3.45)	3.08 (3.08)	3.07 (3.07)	−0.14	2.86
2d	1.68 (1.65)	4.33 (4.43)	3.03 (3.03)	2.96 (2.97)	−0.11	2.65
3d	0.24 (0.23)	1.50 (1.49)	1.67 (1.61)	1.75 (1.68)	−0.05	1.86
1e	1.73 (2.03)	2.99 (2.99)	2.81 (2.81)	2.82 (2.79)	−0.14	2.69

[a] Data taken from work by Siebrand.[67] [b] Data taken from work by Metcalf *et al.*;[68] all the other data are taken from work by Lewis and Kasha.[27] To facilitate the discussion, we calculated the deviation between the computed and the experimental phosphorescence gap at various levels of theory (Fig. 7).

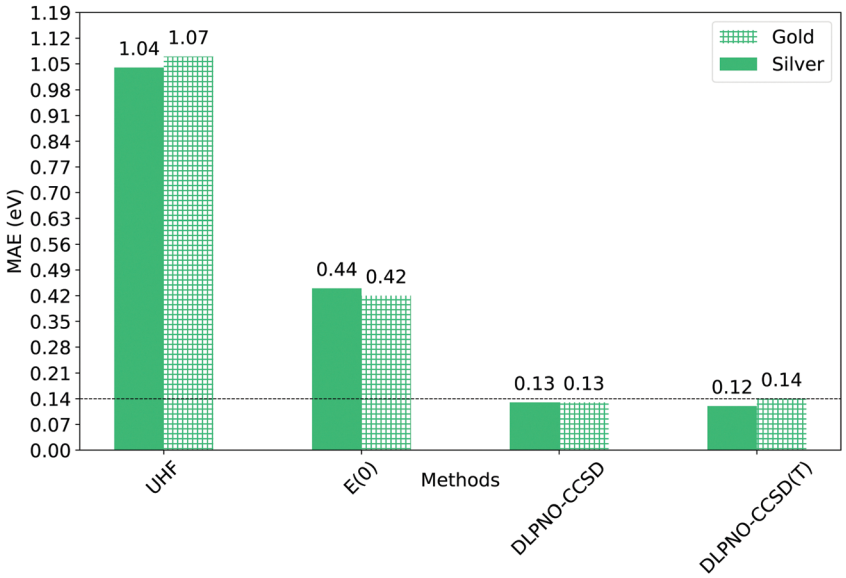

Fig. 7 Mean absolute errors (MAEs) between experimental singlet–triplet gap and computed adiabatic one (ΔE_{00}). ΔE_{00} was calculated using Gold and Silver settings for the dominant ΔE term (Table 3). The corresponding *ZPE*-corrected UHF and QRO energies ($E(0)$) are also shown for comparison.

comparable in all cases. The mean absolute error (MAE) is actually smaller for the Silver settings than for the Gold settings of about 0.02 eV, due to favorable error cancellation. It is also worth mentioning here that ΔZPE ranges from around -0.22 eV to -0.05 eV, and significantly affects the singlet–triplet gap, improving the overall agreement between theory and experiment.

Summarizing the results obtained so far, we can conclude that: (i) the use of the DLPNO approximation enables to simulate the phosphorescence gap of small and medium size aromatic compounds with the same accuracy of the canonical CCSD(T) at a relatively low computational cost, provided that enough care is made in the selection of the technical parameters of the calculation (Gold DLPNO-CCSD(T), Table 3). (ii) For these systems, the effect of the perturbative triples correction on the accuracy is extremely small; this indicates that popular approaches that do not explicitly include this term, such as EOM-CCSD, STEOM-CCSD *etc.*, are expected to provide an adequately accurate description of analogous aromatic compounds in their excited states. (iii) Finally, in spite of the looser thresholds, the Silver methodology (Table 3) provides an accuracy that is comparable to that obtained using the much more conservative Gold settings. This suggests that, by employing the Silver procedure, one may obtain highly accurate results also for large aromatic molecules with a complex electronic structure, as discussed in the next section. It is worth pointing out that since DLPNO-CCSD(T) is a single reference method, it converges on a specific triplet state wave function in case of degenerate or nearly degenerate triplet states. Obviously, this would not affect the singlet–triplet energy gap but it may affect other physical observables.

3.3 The photophysical properties of CDCB compounds

To test the broad applicability of the Silver methodology (Section 2), we applied it to compute the phosphorescence gap of two challenging systems, namely the 4,5-bis(carbazol-9-yl)-1,2-dicyanobenzene (2CzPN) and 1,2,3,5-tetrakis(carbazol-9-yl)-4,6-dicyanobenzene (4CzIPN) (Fig. 8), belonging to carbazolyl dicyanobenzene (CDCB) family. Such systems are charge transfer compounds in which the dicyanobenzene acts as the electron-withdrawing group, while carbazolyl as the electron-donating one, and have found applications as thermally activated

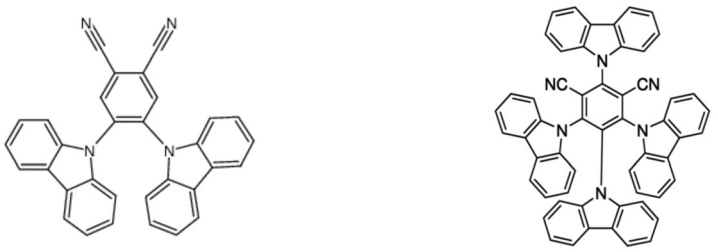

(a) 4,5-Bis(carbazol-9-yl)-1,2-dicyanobenzene (2CzPN)

(b) 1,2,3,5-Tetrakis(carbazol-9-yl)-4,6-dicyanobenzene (4CzIPN)

Fig. 8 CDCB-Based model systems.

Table 5 Adiabatic singlet–triplet gap (ΔE_{00}) at B3LYP and Silver DLPNO-CCSD(T) levels of theory, zero-point differential energy correction (ΔZPE), thermal energy correction at 77 K (Δ_{77K}), energy correction due to solvent effect (Δsolv) and experimental phosphorescence gap (E_{exp}) of compounds 2CzPN and 4CzIPN. All values are reported in eV

Compounds	ΔE_{00} (B3LYP)	ΔE_{00} (Silver)	ΔZPE	Δ_{77K}	Δsolv	E_{exp}
2CzPN	2.44	2.99	−0.11	1.56×10^{-3}	-4.12×10^{-5}	2.75 ref. 111
4CzIPN	2.28	2.94	−0.14	3.52×10^{-3}	-1.20×10^{-1}	2.67 ref. 112

delayed fluorescence (TADF) emitters[103–107] and photocatalysts.[108,109] In particular, among the CDCB compounds, 2CzPN and 4CzIPN have drawn special attention since they represent a viable alternative to transition metal-based chromophores. In fact, they show high photoluminescence quantum yield at room temperature (around 74% for compound 4CzIPN and around 47% for compound 2CzPN).[103] Therefore, they have been widely studied and characterized by both experimental techniques and simulations.

However, the large size of these molecules (54 atoms and 238e$^-$ for compound 2CzPN; 94 atoms and 410e$^-$ for compound 4CzIPN) considerably limits the applicability of post-HF methods for the computation of their photophysical properties, which remains a major challenge. In this context, our DLPNO-CCSD(T)-based protocols may represent a promising tool for the calculation of their photophysical properties.

To test the reliability of DLPNO-CCSD(T), the Silver protocol was used to compute ΔE_{00} of both compounds in toluene at 77 K. Solvent effects were accounted using the conductor-like polarizable continuum model (CPCM) and the *Perturbation Theory Energy* (PTE) approximation which is the default scheme of ORCA 5.0.1 for the treatment of the coupled-cluster Lagrangian of implicitly solvated systems. Although less crude approximations such as PTE(S) and PTES are already available in ORCA 5.0.1 (see ORCA 5.0.1 manual for further details), PTE scheme proved to be highly reliable for a wide variety of neutral organic solutes with deviations from PTE(S) and PTES energies of only few tenths of kcal mol^{-1}.[110] The results are shown in Table 5 alongside with the corresponding experimental values.

The data reported in Table 5 demonstrate that the Silver DLPNO-CCSD(T) approach returns highly accurate results also for these systems. For the 2CzPN compound, the adiabatic Silver singlet–triplet gap is 2.99 eV, while the experimental value is 2.75 eV. Thus, the deviation between theory and experiment in this case is only slightly larger than that obtained for the other aromatic compounds studied in this work. For the sake of comparison, the corresponding B3LYP value is 2.44 eV. Concerning instead the 4CzIPN compound, the Silver DLPNO-CCSD(T), the experimental and the B3LYP singlet–triplet gap are 2.94 eV, 2.67 eV and 2.28 eV, respectively. Hence, in this case, the DLPNO-CCSD(T)-based method is more accurate than B3LYP by 0.12 eV.

To further validate the reliability of Silver method, we also calculate the phosphorescence spectrum and rate constants of 2CzPN within a path integral framework, as detailed in the Section 2.4. The computed spectrum reported in Fig. 9 results from the average of spectra of the first three roots obtained from SOC-TDDFT, which approximately correspond to the three spin sub-levels of the first triplet; the experimental one instead has been recorded by Hosokai *et al.* in toluene at 77 K.

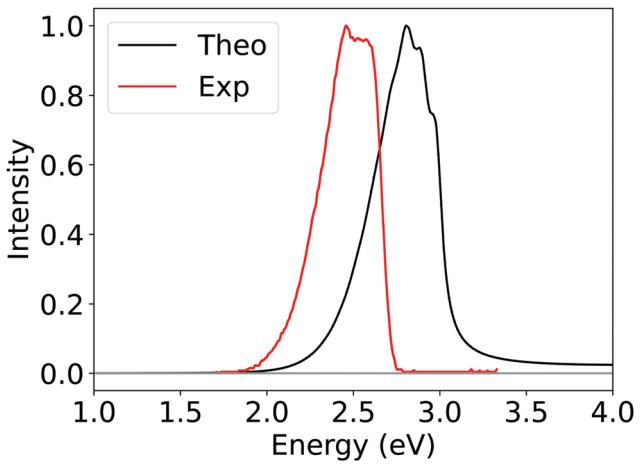

Fig. 9 Computed phosphorescence spectrum of 2CzPN obtained by employing Silver DLPNO-CCSD(T) ΔE (black curve) and experimental phosphorescence spectrum (red curve) recorded by Hosokai *et al.* See text for details.[113]

Considering the challenging nature of this system, the qualitative agreement observed between the computed and experimental spectra is remarkable, even though the former is blue-shifted by around 0.3 eV. At least part of this effect should originate from the implicit solvation model employed. Further and deeper investigations, beyond the scope of this work, should be conducted in order to address this phenomenon.

Importantly, the theoretical average phosphorescence rate constant (3.49 s^{-1}) is of the same order of the experimental phosphorescence rate constant (9.09 s^{-1})[107] and well within the experimental error. The latter refers to a phosphorescence experiment in a 1,3-bis(9-carbazolyl)benzene (mCP) film at 80 K.

4 Conclusions

We assessed the accuracy and efficiency of the DLPNO-CCSD(T) method for the calculation of phosphorescence energies, spectra and rate constants of aromatics.

Initially, an extensive analysis of the accuracy and computational cost of the methodology for the calculation of singlet and triplet energies of aromatic molecules was conducted, in relation to the main technical parameters of the calculation (basis

set, triples correction approximation, dimension of PNOs space).

Our analysis revealed that large basis sets with cardinality $N \geq 3$ are required to reduce the error below 0.09 eV with respect to the complete basis set limit. Larger basis sets and extrapolation techniques are needed to reach chemical accuracy (0.04 eV). In addition, it was found that aug-cc-pVNZ basis sets family does not provide any advantage in terms of accuracy with respect to cc-pVNZ basis sets one. In contrast, it dramatically increases the computational cost of the calculations.

Remarkably enough, the contribution of the perturbative triples correction to the gap was found to be rather small, inasmuch the deviation of the DLPNO-CCSD gap from the DLPNO-CCSD(T) one is below 0.09 eV. This suggests that methods that do not include a triples contribution may still be suitable for predicting the photophysical properties of aromatics.

The convergence of the DLPNO-CCSD(T) electronic energy for triplet and singlet states with respect to the key DLPNO parameters was also investigated in detail. It was found that standard thresholds are adequate for the description aromatic systems.

These results were used to define two DLPNO-CCSD(T) settings for the calculation of singlet–triplet gaps of aromatics, differing for their accuracy and computational cost. The ''Gold'' DLPNO-CSSD(T) settings provide results that are at convergence with respect to all the technical parameters of the calculation. It provides a MAE that is the same as the canonical CCSD(T) one (0.14 eV) with respect to the experimental reference data. This approach is applicable to medium-sized molecules. For larger systems, the cost-effective ''Silver'' DLPNO-CCSD(T) settings should be used. These settings provide MAEs with respect to the experimental phosphorescence gap that are still comparable to the ''Gold'' settings, enabling highly accurate simulations of large aromatic molecules.

Finally, the Silver DLPNO-CCSD(T) method was used to compute the phosphorescence gap, spectra and rate constants of prototype CDCB compounds in toluene. A very good agreement was found between theory and experiment, which suggests that our computational protocol is potentially broadly applicable. This work opens new avenues for the calculation of the photophysical properties of aromatic compounds.

Conflicts of interest

There are no conflicts to declare.

References

1 H.-G. Franck and J. W. Stadelhofer, *Industrial Aromatic Chemistry*. 1998.
2 P. K. Seshan, The absorption spectra of some aromatic compounds, *Proc. Indian Acad. Sci.*, 1936, **3**, 172–187.
3 D. C. Northrop and O. Simpson, Electronic properties of aromatic hydrocarbons. iv. photo-electric effects, *Proc. R. Soc. London, Ser. A*, 1958, **244**, 377–389.
4 E. Clar, *The Electrical Conductivity of Aromatic Hydrocarbons*, Berlin, Heidelberg: Springer Berlin Heidelberg, 1964, pp. 118–118.
5 A. J. Epstein, S. Etemad, A. F. Garito and A. J. Heeger, Metal–insulator transition and antiferromagnetism in a one-dimensional organic solid, *Phys. Rev. B: Condens. Matter Mater. Phys.*, 1972, **5**, 952–977.
6 M. Weger, *The Electrical Conductivity of TTF–TCNQ and Related Compounds*. Boston, MA: Springer US, 1979, pp. 123–134.
7 J. Ferraris, D. O. Cowan, V. Walatka and J. H. Perlstein, Electron transfer in a new highly conducting donor-acceptor complex, *J. Am. Chem. Soc.*, 1973, **95**(3), 948–949.
8 B. O'Regan and M. Graetzel, A low-cost, high-efficiency solar cell based on dye-sensitized colloidal TiO_2 films, *Nature*, 1991, **353**, 737–740.
9 A. Carella, F. Borbone and R. Centore, Research progress on photosensitizers for dssc, *Front. Chem.*, 2018, **6**, 481.
10 A. Mishra, M. Fischer and P. Bäuerle, Metal-free organic dyes for dye-sensitized solar cells: from structure: property relationships to design rules, *Angew. Chem., Int. Ed.*, 2009, **48**(14), 2474–2499.
11 J. Albero, P. Atienzar, A. Corma and H. Garcia, Efficiency records in mesoscopic dye-sensitized solar cells, *Chem. Record*, 2015, **15**(4), 803–828.
12 T. Higashino and H. Imahori, Porphyrins as excellent dyes for dye-sensitized solar cells: recent developments and insights, *Dalton Trans.*, 2015, **44**, 448–463.
13 C.-P. Lee, C.-T. Li and K.-C. Ho, Use of organic materials in dye-sensitized solar cells, *Mater. Today*, 2017, **20**(5), 267–283.
14 T. El-Agez, S. Taya, K. Elrefi and M. Abdel latif, Dye-sensitized solar cells using some organic dyes as photosensitizers, *Opt. Appl.*, 2014, **44**, 345–351.
15 D. Lee, M. J. Lee, H. M. Song, B. Song, K. Seo, M. Pastore, C. Anselmi, S. Fantacci, F. Angelis, M. Nazeeruddin and M. Graetzel, Organic dyes incorporating low-band-gap chromophores based on -extended benzothiadiazole for dye-sensitized solar cells, *Dyes Pigm.*, 2011, **91**, 192–198.
16 M. A. Filatov, Heavy-atom-free bodipy photosensitizers with intersystem crossing mediated by intramolecular photoinduced electron transfer, *Org. Biomol. Chem.*, 2020, **18**, 10–27.
17 C. W. Tang and S. A. VanSlyke, Organic electroluminescent diodes, *Appl. Phys. Lett.*, 1987, **51**(12), 913–915.
18 Y. Karzaki, Organic light emitting diodes: devices and applications, *J. Mater. Environ. Sci.*, 2014, **5**, 1–12.
19 J. Y. Xue, T. Izumi, A. Yoshii, K. Ikemoto, T. Koretsune, R. Akashi, R. Arita, H. Taka, H. Kita, S. Sato and H. Isobe, Aromatic hydrocarbon macrocycles for highly efficient organic light-emitting devices with single-layer architectures, *Chem. Sci.*, 2016, **7**, 896–904.

20 Y. Qin, G. Li, T. Qi and H. Huang, Aromatic imide/amide-based organic small-molecule emitters for organic light-emitting diodes, *Mater. Chem. Front.*, 2020, **4**, 1554–1568.
21 T. Itoh, Fluorescence and Phosphorescence from Higher Excited States of Organic Molecules, *Chem. Rev.*, 2012, **112**(8), 4541–4568.
22 S. Naskar and M. Das, Singlet and triplet excited state energy ordering in cyclopenta-fused polycyclic aromatic hydrocarbons (cp-pahs) suitable for energy harvesting: an exact model and tddft study, *ACS Omega*, 2017, **2**(5), 1795–1803.
23 E. V. Donckt, R. Dramaix, J. Nasielski and C. Vogels, Photochemistry of aromatic compounds. part 1. acid-base properties of singlet and triplet excited states of pyrene derivatives and aza-aromatic compounds, *Trans. Faraday Soc.*, 1969, **65**, 3258–3262.
24 F. Masetti, U. Mazzucato and J. Birks, Photophysical behaviour of azaphenanthrenes, *Chem. Phys.*, 1975, **9**(3), 301–306.
25 H. LöfÅs, B. O. Jahn, J. Wärnå, R. Emanuelsson, R. Ahuja, A. Grigoriev and H. Ottosson, A computational study of potential molecular switches that exploit baird's rule on excited-state aromaticity and antiaromaticity, *Faraday Discuss.*, 2014, **174**, 105–124.
26 Z. Tu, G. Han, T. Hu, R. Duan and Y. Yi, Nature of the lowest singlet and triplet excited states of organic thermally activated delayed fluorescence emitters: a self-consistent quantum mechanics/embedded charge study, *Chem. Mater.*, 2019, **31**(17), 6665–6671.
27 G. N. Lewis and M. Kasha, Phosphorescence and the Triplet State, *J. Am. Chem. Soc.*, 1944, **66**(12), 2100–2116.
28 R. H. Friend, R. W. Gymer, A. B. Holmes, J. H. Burroughes, R. N. Marks, C. Taliani, D. D.-C. Bradley, D. A.-D. Santos, J. L. Brédas, M. Lögdlund and W. R. Salaneck, Electroluminescence in conjugated polymers, *Nature*, 1999, **397**(6715), 121–128.
29 D. J. Gibbons, A. Farawar, P. Mazzella, S. Leroy-Lhez and R. M. Williams, Making triplets from photo-generated charges: observations, mechanisms and theory, *Photochem. Photobiol. Sci.*, 2020, **19**, 136–158.
30 W. Paa, J.-P. Yang and S. Rentsch, Ultrafast intersystem crossing in thiophene oligomers investigated by fs-pump-probe spectroscopy, *Synth. Metals*, 2001, **119**(1), 525–526. Proceedings of the International Conference on Science and technology of Synthetic Metals.
31 S. Hirata, Recent advances in materials with room-temperature phosphorescence: photophysics for triplet exciton stabilization, *Adv. Opt. Mater.*, 2017, **5**(17), 1700116.
32 J. P. Zobel, J. J. Nogueira and L. González, Mechanism of ultrafast intersystem crossing in 2-nitronaphthalene, *Chem. – Eur. J.*, 2018, **24**(20), 5379–5387.
33 R. A. Vogt, C. Reichardt and C. E. Crespo-Hernández, Excited-state dynamics in nitro-naphthalene derivatives: intersystem crossing to the triplet manifold in hundreds of femtoseconds, *J. Phys. Chem. A*, 2013, **117**(30), 6580–6588.
34 E. Collado-Fregoso, J. S. Zugazagoitia, E. F. Plaza-Medina and J. Peon, Excited-state dynamics of nitrated push–pull molecules: the importance of the relative energy of the singlet and triplet manifolds, *J. Phys. Chem. A*, 2009, **113**(48), 13498–13508.
35 R. W. Yip, D. K. Sharma, R. Giasson and D. Gravel, Picosecond excited-state absorption of alkylnitrobenzenes in solution, *J. Phys. Chem.*, 1984, **88**, 5770–5772.
36 T. Schmierer, G. Ryseck, N. Villnow, T. Regner and P. Gilch, Kasha or state selective behavior in the photochemistry of *ortho*-nitrobenzaldehyde, *Photochem. Photobiol. Sci.*, 2012, **11**, 1313–1321.
37 N. J. Turro, *Modern Molecular Photochemistry*. Mill-Valley, California, University Science Books, 1991.
38 S. G. Cohen and H. M. Chao, Photoreduction of aromatic ketones by amines. studies of quantum yields and mechanism, *J. Am. Chem. Soc.*, 1968, **90**(1), 165–173.
39 S. Hirayama, Photochemical reactions of aromatic aldehydes and ketones: higher triplet state reactions and radiationless transitions, *Rev. Phys. Chem. Jpn.*, 1972, **42**(1), 49–74.
40 N. C. Baird, Quantum organic photochemistry. II. Resonance and aromaticity in the lowest $3\pi\cdots\pi^*$ state of cyclic hydrocarbons, *J. Am. Chem. Soc.*, 1972, **94**, 4941–4948.
41 L. J. Karas, C.-H. Wu, H. Ottosson and J. I. Wu, Electron-driven proton transfer relieves excited-state antiaromaticity in photoexcited dna base pairs, *Chem. Sci.*, 2020, **11**, 10071–10077.
42 L. J. Karas and J. I.-C. Wu, 10 – antiaromatic compounds: a brief history, applications, and the many ways they escape antiaromaticity, in *Aromaticity*, ed. I. Fernandez, Elsevier, 2021, pp. 319–338.
43 T. J. Zuehlsdorff, N. D. Hine, M. C. Payne and P. D. Haynes, Linear-scaling time-dependent density-functional theory beyond the Tamm-Dancoff approximation: obtaining efficiency and accuracy with in situ optimised local orbitals, *J. Chem. Phys.*, 2015, **28**(43(20)), 204107.
44 M. J.-G. Peach and D. J. Tozer, Overcoming low orbital overlap and triplet instability problems in tddft, *J. Phys. Chem. A*, 2012, **116**(39), 9783–9789.
45 A. Dreuw and M. Head-Gordon, Single-reference ab initio methods for the calculation of excited states of large molecules, *Chem. Rev.*, 2005, **105**(11), 4009–4037.
46 C. Jamorski, M. E. Casida and D. R. Salahub, Dynamic polarizabilities and excitation spectra from a molecular implementation of time-dependent density-functional response theory: N2 as a case study, *J. Chem. Phys.*, 1996, **104**(13), 5134–5147.
47 R. Bauernschmitt and R. Ahlrichs, Treatment of electronic excitations within the adiabatic approximation of time dependent density functional theory, *Chem. Phys. Lett.*, 1996, **256**(4), 454–464.
48 S. Hirata and M. Head-Gordon, Time-dependent density functional theory within the tamm-dancoff approximation, *Chem. Phys. Lett.*, 1999, **314**(3), 291–299.
49 M. E. Casida, F. Gutierrez, J. Guan, F.-X. Gadea, D. Salahub and J.-P. Daudey, Charge-transfer correction for improved

time-dependent local density approximation excited-state potential energy curves: analysis within the two-level model with illustration for h2 and lih, *J. Chem. Phys.*, 2000, **113**(17), 7062–7071.

50 F. Cordova, L. J. Doriol, A. Ipatov, M. E. Casida, C. Filippi and A. Vela, Troubleshooting time-dependent density-functional theory for photochemical applications: oxirane, *J. Chem. Phys.*, 2007, **127**(16), 164111.

51 O. B. Lutnæs, T. Helgaker and M. Jaszuński, Spin-spin coupling constants and triplet instabilities in kohn-sham theory, *Mol. Phys.*, 2010, **108**(19–20), 2579–2590.

52 J. S. Sears, T. Koerzdoerfer, C.-R. Zhang and J.-L. Brédas, Communication: orbital instabilities and triplet states from time-dependent density functional theory and long-range corrected functionals, *J. Chem. Phys.*, 2011, **135**(15), 151103.

53 S. Grimme and F. Neese, Double-hybrid density functional theory for excited electronic states of molecules, *J. Chem. Phys.*, 2007, **127**(15), 154116.

54 M. Casanova-Páez and L. Goerigk, Assessing the tamm-dancoff approximation, singlet–singlet, and singlet–triplet excitations with the latest long-range corrected double-hybrid density functionals, *J. Chem. Phys.*, 2020, **153**(6), 064106.

55 M. Casanova-Páez and L. Goerigk, Time-dependent long-range-corrected double-hybrid density functionals with spin-component and spin-opposite scaling: a comprehensive analysis of singlet-singlet and singlet–triplet excitation energies, *J. Chem. Theory Comput.*, 2021, **17**(8), 5165–5186.

56 L. Wilbraham, C. Adamo and I. Ciofini, Communication: evaluating non-empirical double hybrid functionals for spin-state energetics in transition-metal complexes, *J. Chem. Phys.*, 2018, **148**(4), 041103.

57 P. M. Zimmerman, Singlet–triplet gaps through incremental full configuration interaction, *J. Phys. Chem. A*, 2017, **121**(24), 4712–4720.

58 B. Hajgató, D. Szieberth, P. Geerlings, F. De Proft and M. S. Deleuze, A benchmark theoretical study of the electronic ground state and of the singlet–triplet split of benzene and linear acenes, *J. Chem. Phys.*, 2009, **131**(22), 224321.

59 B. Nebgen, *Dataset of singlet and triplet energies and forces for organic molecules*, 2021.

60 J. Westermayr and P. Marquetand, Machine learning for electronically excited states of molecules, *Chem. Rev.*, 2021, **121**(16), 9873–9926.

61 A. E. Sifain, L. Lystrom, R. A. Messerly, J. S. Smith, B. Nebgen, K. Barros, S. Tretiak, N. Lubbers and B. J. Gifford, Predicting phosphorescence energies and inferring wavefunction localization with machine learning, *Chem. Sci.*, 2021, **12**, 10207–10217.

62 C. Riplinger, P. Pinski, U. Becker, E. F. Valeev and F. Neese, Sparse maps—a systematic infrastructure for reduced-scaling electronic structure methods. ii. linear scaling domain based pair natural orbital coupled cluster theory, *J. Chem. Phys.*, 2016, **144**(2), 024109.

63 C. Riplinger, B. Sandhoefer, A. Hansen and F. Neese, Natural triple excitations in local coupled cluster calculations with pair natural orbitals, *J. Chem. Phys.*, 2013, **139**(13), 134101.

64 P. Pulay, S. Saebo and W. Meyer, An efficient reformulation of the closed-shell self-consistent electron pair theory, *J. Chem. Phys.*, 1984, **81**(4), 1901–1905.

65 M. Schütz and H.-J. Werner, Local perturbative triples correction (T) with linear cost scaling, *Chem. Phys. Lett.*, 2000, **318**(4), 370–378.

66 M. Schütz and H.-J. Werner, Low-order scaling local electron correlation methods. iv. linear scaling local coupled-cluster (LCCSD), *J. Chem. Phys.*, 2001, **114**(2), 661–681.

67 W. Siebrand, Radiationless transitions in polyatomic molecules. ii. triplet-ground-state transitions in aromatic hydrocarbons, *J. Chem. Phys.*, 1967, **47**(7), 2411–2422.

68 J. Metcalfe, M. G. Rockley and D. Phillips, Single–triplet absorption spectra of substituted benzenes, *J. Chem. Soc., Faraday Trans. 2*, 1974, **70**, 1660–1666.

69 F. Neese, The orca program system, *Wiley Interdiscip. Rev.: Comput. Mol. Sci.*, 2012, **2**(1), 73–78.

70 S. Grimme and M. Steinmetz, Effects of london dispersion correction in density functional theory on the structures of organic molecules in the gas phase, *Phys. Chem. Chem. Phys.*, 2013, **15**, 16031–16042.

71 S. Grimme, Density functional theory with london dispersion corrections, *Wiley Interdiscip. Rev.: Comput. Mol. Sci.*, 2011, **1**(2), 211–228.

72 S. Grimme, A. Hansen, J. G. Brandenburg and C. Bannwarth, Dispersion-corrected mean-field electronic structure methods, *Chem. Rev.*, 2016, **116**(9), 5105–5154.

73 M. S. Deleuze, M. G. Giuffreda and J.-P. François, Valence one-electron and shake-up ionization bands of carbon clusters. II. The C_n (n = 5, 7, 9, 11) rings, *J. Phys. Chem. A*, 2002, **106**(23), 5626–5637.

74 J. M.-L. Martin, A. Sundermann, P. L. Fast and D. G. Truhlar, Thermochemical analysis of core correlation and scalar relativistic effects on molecular atomization energies, *J. Chem. Phys.*, 2000, **113**(4), 1348–1358.

75 F. Neese, Software update: the orca program system, version 4.0, *Wiley Interdiscip. Rev.: Comput. Mol. Sci.*, 2018, **8**(1), e1327.

76 F. Weigend, M. Häser, H. Patzelt and R. Ahlrichs, Ri-mp2: optimized auxiliary basis sets and demonstration of efficiency, *Chem. Phys. Lett.*, 1998, **294**(1), 143–152.

77 K. Eichkorn, O. Treutler, H. Öhm, M. Häser and R. Ahlrichs, Auxiliary basis sets to approximate coulomb potentials, *Chem. Phys. Lett.*, 1995, **240**(4), 283–290.

78 M. Saitow, U. Becker, C. Riplinger, E. F. Valeev and F. Neese, A new near-linear scaling, efficient and accurate, open-shell domain-based local pair natural orbital coupled cluster singles and doubles theory, *J. Chem. Phys.*, 2017, **146**(16), 164105.

79 D. G. Liakos, Y. Guo and F. Neese, Comprehensive benchmark results for the domain based local pair natural orbital coupled cluster method (DLPNO-CCSD(T)) for

closed- and open-shell systems, *J. Phys. Chem. A*, 2020, **124**(1), 90–100.

80 F. Neese, Importance of direct spin–spin coupling and spin–flip excitations for the zero-field splittings of transition metal complexes: a case study, *J. Am. Chem. Soc.*, 2006, **128**(31), 10213–10222.

81 J.-L. Heully and J.-P. Malrieu, What would be the most relevant transcription of a CCSD(T) method into a dressed sdci matrix?, *J. Mol. Struct.: THEOCHEM*, 2006, **768**(1), 53–62.

82 M. Schütz, Low-order scaling local electron correlation methods. iii. linear scaling local perturbative triples correction (T), *J. Chem. Phys.*, 2000, **113**(22), 9986–10001.

83 Y. Guo, C. Riplinger, U. Becker, D. G. Liakos, Y. Minenkov, L. Cavallo and F. Neese, Communication: an improved linear scaling perturbative triples correction for the domain based local pair-natural orbital based singles and doubles coupled cluster method [DLPNO-CCSD(T)], *J. Chem. Phys.*, 2018, **148**(1), 011101.

84 T. H. Dunning, Gaussian basis sets for use in correlated molecular calculations. i. the atoms boron through neon and hydrogen, *J. Chem. Phys.*, 1989, **90**(2), 1007–1023.

85 R. A. Kendall, T. H. Dunning and R. J. Harrison, Electron affinities of the first-row atoms revisited. systematic basis sets and wave functions, *J. Chem. Phys.*, 1992, **96**(9), 6796–6806.

86 A. Karton and J. M.-L. Martin, Comment on: Estimating the Hartree-Fock limit from finite basis set calculations, *Theor. Chem. Acc.*, 2006, **115**, 330–333.

87 S. Zhong, E. C. Barnes and G. A. Petersson, Uniformly convergent n-tuple-augmented polarized (nzap) basis sets for complete basis set extrapolations. i. self-consistent field energies, *J. Chem. Phys.*, 2008, **129**(18), 184116.

88 D. G. Truhlar, Basis-set extrapolation, *Chem. Phys. Lett.*, 1998, **294**(1), 45–48.

89 T. Helgaker, W. Klopper, H. Koch and J. Noga, Basis-set convergence of correlated calculations on water, *J. Chem. Phys.*, 1997, **106**(23), 9639–9646.

90 A. Halkier, T. Helgaker, P. Jørgensen, W. Klopper, H. Koch, J. Olsen and A. K. Wilson, Basis-set convergence in correlated calculations on Ne, N_2, and H_2O, *Chem. Phys. Lett.*, 1998, **286**(3), 243–252.

91 F. Neese and E. F. Valeev, Revisiting the atomic natural orbital approach for basis sets: robust systematic basis sets for explicitly correlated and conventional correlated ab initio methods?, *J. Chem. Theory Comput.*, 2011, **7**(1), 33–43.

92 A. Altun, F. Neese and G. Bistoni, Extrapolation to the limit of a complete pair natural orbital space in local coupled-cluster calculations, *J. Chem. Theory Comput.*, 2020, **16**(10), 6142–6149.

93 A. Altun, S. Ghosh, C. Riplinger, F. Neese and G. Bistoni, Addressing the system-size dependence of the local approximation error in coupled-cluster calculations, *J. Phys. Chem. A*, 2021, **125**(45), 9932–9939.

94 L. Goerigk, A. Hansen, C. Bauer, S. Ehrlich, A. Najibi and S. Grimme, A look at the density functional theory zoo with the advanced gmtkn55 database for general main group thermochemistry, kinetics and noncovalent interactions, *Phys. Chem. Chem. Phys.*, 2017, **19**, 32184–32215.

95 B. de Souza, F. Neese and R. Izsák, On the theoretical prediction of fluorescence rates from first principles using the path integral approach, *J. Chem. Phys.*, 2018, **148**(3), 034104.

96 B. de Souza, G. Farias, F. Neese and R. Izsák, Predicting phosphorescence rates of light organic molecules using time-dependent density functional theory and the path integral approach to dynamics, *J. Chem. Theory Comput.*, 2019, **15**(3), 1896–1904.

97 B. Helmich-Paris, B. de Souza, F. Neese and R. Izsák, An improved chain of spheres for exchange algorithm, *J. Chem. Phys.*, 155, 10, 104109, 2021. Publisher: American Institute of Physics.

98 R. Cammi and B. Mennucci, Linear response theory for the polarizable continuum model, *J. Chem. Phys.*, 1999, **110**(20), 9877–9886.

99 F. Neese, Efficient and accurate approximations to the molecular spin-orbit coupling operator and their use in molecular g-tensor calculations, *J. Chem. Phys.*, 2005, **122**(3), 034107.

100 C. U. Ibeji and D. Ghosh, Singlet–triplet gaps in polyacenes: a delicate balance between dynamic and static correlations investigated by spin-flip methods, *Phys. Chem. Chem. Phys.*, 2015, **17**, 9849–9856.

101 S. Mallick, P. K. Rai and P. Kumar, Accurate estimation of singlet–triplet gap of strongly correlated systems by CCSD(T) method using improved orbitals, *Comput. Theoretical Chem.*, 2021, **1202**, 113326.

102 D. G. Liakos, M. Sparta, M. K. Kesharwani, J. M.-L. Martin and F. Neese, Exploring the accuracy limits of local pair natural orbital coupled-cluster theory, *J. Chem. Theory Comput.*, 2015, **11**(4), 1525–1539.

103 H. Uoyama, K. Goushi, K. Shizu, H. Nomura and C. Adachi, Highly efficient organic light-emitting diodes from delayed fluorescence, *Nature*, 2012, **492**(7428), 234–238. Funding Information: Acknowledgements This work was supported by the Funding Program for World-Leading Innovative R D on Science and Technology (FIRST) and the International Institute for Carbon Neutral Energy Research (WPI-I2CNER), sponsored by the Japanese Ministry of Education, Culture, Sports, Science and Technology. H.U. acknowledges a Grand-in-Aid for JSPS Fellows. We thank H. Nakanotani, J.-I. Nishide, and H. Miyazaki for their assistance with this research. We also thank K. Tokumaru, H. Sasabe, W. Potscavage and M. Gábor for their assistance with preparation of this manuscript.

104 F. B. Dias, T. J. Penfold and A. P. Monkman, Photophysics of thermally activated delayed fluorescence molecules, *Methods Appl. Fluoresc.*, 2017, **5**(1), 012001.

105 F. Rodella, S. Bagnich, E. Duda, T. Meier, J. Kahle, S. Athanasopoulos, A. Köhler and P. Strohriegl, High triplet energy host materials for blue tadf oleds—a tool box approach, *Front. Chem.*, 2020, **8**, 657.

106 B. Wex and B. R. Kaafarani, Perspective on carbazole-based organic compounds as emitters and hosts in tadf applications, *J. Mater. Chem. C*, 2017, **5**, 8622–8653.
107 E. Duda, *What Controls Thermally Activated Delayed Fluorescence in Guest-Host Systems for Organic Light-Emitting Diodes? PhD thesis*, Bayreuth, 2021.
108 E. Speckmeier, T. G. Fischer and K. Zeitler, A toolbox approach to construct broadly applicable metal-free catalysts for photoredox chemistry: deliberate tuning of redox potentials and importance of halogens in donor-acceptor cyanoarenes, *J. Am. Chem. Soc.*, 2018, **140**(45), 15353–15365.
109 M. A. Bryden and E. Zysman-Colman, Organic thermally activated delayed fluorescence (tadf) compounds used in photocatalysis, *Chem. Soc. Rev.*, 2021, **50**, 7587–7680.
110 M. Garcia-Ratés, U. Becker and F. Neese, Implicit solvation in domain based pair natural orbital coupled cluster (dlpno-ccsd) theory, *J. Comput. Chem.*, 2021, **42**(27), 1959–1973.
111 A. Rodriguez-Serrano, F. Dinkelbach and C. M. Marian, Intersystem crossing processes in the 2czpn emitter: a dft/mrci study including vibrational spin-orbit interactions, *Phys. Chem. Chem. Phys.*, 2021, **23**, 3668–3678.
112 H. Noda, X. Chen, H. Nakanotani, T. Hosokai, M. Miyajima, N. Notsuka, Y. Kashima, J. Brédas and C. Adachi, Critical role of intermediate electronic states for spin-flip processes in charge-transfer-type organic molecules with multiple donors and acceptors, *Nat. Mater.*, 2019, **18**(10), 1084–1090.
113 T. Hosokai, H. Matsuzaki, H. Nakanotani, K. Tokumaru, T. Tsutsui, A. Furube, K. Nasu, H. Nomura, M. Yahiro and C. Adachi, Evidence and mechanism of efficient thermally activated delayed fluorescence promoted by delocalized excited states, *Sci. Adv.*, 2017, **3**(5), e1603282.